

Review

Important Approaches to Enhance Reverse Osmosis (RO) Thin Film Composite (TFC) Membranes Performance

Ahmed Al Mayyahi

Department of Chemical Engineering, University of Missouri, Columbia, MO 65211, USA;
aaakz5@mail.missouri.edu or sumrabm@yahoo.com

Received: 17 July 2018; Accepted: 9 August 2018; Published: 21 August 2018



Abstract: Thin film composite (TFC) membrane, which consists of polyamide (PA) active film rests on porous support layer, has been the major type of reverse osmosis (RO) membrane since its development by Cadotte in the 1970s, and has been remarkably used to produce clean water for human consumption and domestic utilization. In the past 30 years, different approaches have been exploited to produce the TFC membrane with high water flux, excellent salt rejection, and better chlorine/fouling resistance. In this brief review, we classify the techniques that have been utilized to improve the RO-TFC membrane properties into four categories: (1) Using alternative monomers to prepare the active layer; (2) modification of membrane surface; (3) optimization of polymerization reactions; and (4) incorporation of nanoparticles (NPs) into the membrane PA layer. This review can provide insights to guide future research and further propel the RO TFN membrane.

Keywords: nanoparticles (NPs); thin film composite (TFC); interfacial polymerization (IP); surface modification

1. Introduction

Because of the rapid growth of the world population and rising water needs, water shortage problems have become dominant [1,2]. In the last century, as the global population quadrupled, the world water demand has increased sevenfold. The problem of water scarcity is not only a problem of appropriate techniques, but also a social and educational problem relying on national and global endeavors as well as on technical solutions [3]. To address water shortage problems, many techniques have been developed including distillation, membrane reverse osmosis (RO), mechanical vapor pressure compression, electrodialysis and nanofiltration processes [4]. Membrane separation processes are gaining global acceptance in both water treatment and desalination due to their simplicity and relatively low cost compared to other treatment technologies [5]. RO membranes can be effectively used to remove salts and other pollutants from brackish water [6]. The water is transferred through the RO membrane by diffusion [7], while the salt is rejected by size exclusion and repulsion electrostatic force between the membrane surface and dissolved ions, which is caused by charge difference [8,9]. For efficient desalination, the membranes must be permeable to water, impermeable to solutes, and capable of tolerating high operating pressures [9].

The first work on RO membranes was initiated by Reid and co-workers [10] in the early 1950s, when they successfully fabricated an active cellulose acetate membrane to remove salt from water. The membrane exhibited efficient desalination (salt rejection: 96%), but water flux through the membrane was significantly low. Researches continued at the University of California, Los Angeles, with the concern of improving water flux without sacrificing salt rejection [11]. In 1961, Sourirajain [12] enhanced membrane flux by increasing cellulosic film porosity through using pore-forming monomers.

However, cellulose acetate membrane has limited applications due to its weak chemical resistance and low thermal stability [13,14]. Thus, many studies were conducted to produce a membrane with better characteristics. In 1979, Burns and coworkers [15] suggested the use of aromatic polyamide (PA) membrane, which is recognized by its cheap price and high temperature tolerance, as an alternative [15,16]. Though water permeability by this membrane is less than that of cellulose acetate membrane, their salt rejection is higher.

A major breakthrough in the field of RO is the development of PA thin film composite (TFC) membrane. This membrane consists of two layers, the top is an active PA film prepared by the reaction between *m*-Phenylenediamine (MPD) and trimesoyl chloride (TMC) on a microporous polysulfone support (PSU), the bottom layer [17,18], as shown in Figure 1. Water flux through the composite membranes depends on the hydrophilicity of the membrane surface and the characteristics of the porous support layer, while salt rejection relies on the surface charges and PA structure [14].

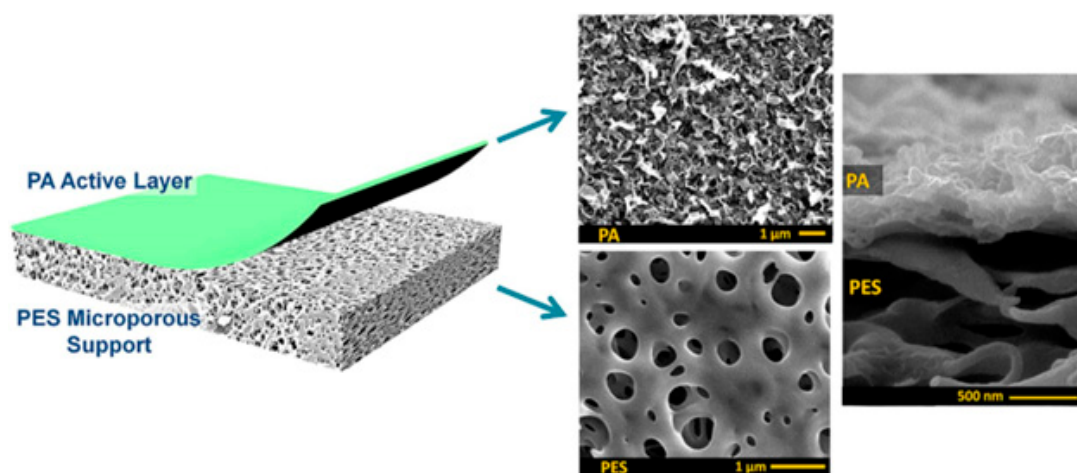


Figure 1. Polyamide thin film composite membrane, reproduced with permission from Khorshidi et al. [18].

Several state-of-the-art reviews have been published to highlight the types of RO-TFC membranes and their performance. For instance, Yin et al. [19] detailed the benefits of incorporating various nanoparticles on the membrane's water flux, salt rejection, chlorine resistance, and antifouling properties. Another review by Xu et al. [20] discussed the influences of sub-layer adjustment on pressure gradient across the membrane and subsequent performance. Recently, Gohil et al. [21] reviewed the systematic development of TFC membranes with their structural composition and separation characteristics, including the effects of various additives and IP reaction parameters. However, until now, there has been no clear classification of the approaches that have been used to enhance RO-TFC membranes properties. Thus, the objective of this brief review is to fill this gap in literature and provide new insights for readers to improve their knowledge in this field.

2. Using Alternative Monomers to Prepare the Active Layer

Because membrane performance is substantially dependent on a thin film structure and its chemical properties, different monomers have been used to prepare the PA, as shown in Table 1. For example, Li et al. [22] used three different isomeric biphenyl acid chlorides (*mm*-BTCE, *om*-BTCE, *op*-PTCE) to react, separately, with *m*-phenylenediamine (MPD) on a porous support. Results indicated that the membrane prepared from *op*-PTCE exhibited higher water flux and lower salt rejection, while those prepared from *mm*-BTCE and *om*-BTCE showed lower water flux and higher salt rejection. The reason behind permeability enhancement could be due to the high density of the carboxylic acid group on the membrane prepared from *op*-PTCE, which led to better contact with water molecules. On the other hand, the higher salt rejection might be because of the thicker PA layer produced by

using *mm*-BTCE and *om*-BTCE. Another study was reported by Wang et al. [23] in which introducing 3,5 diamino-*N*-(4-2-aminophenyl)-benzamide (DABA) as a monomer to react with TMC through interfacial polymerization resulted in a more hydrophilic, thinner, and smoother membrane.

Table 1. Reported monomers for synthesis of polyamide composite membranes.

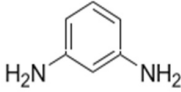
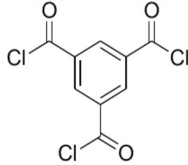
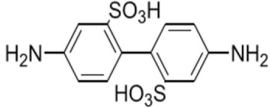
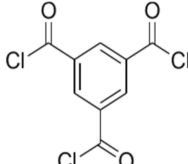
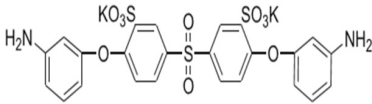
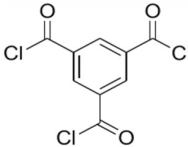
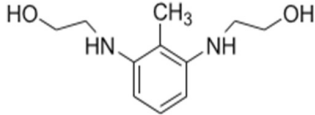
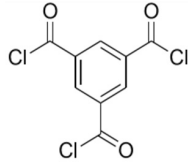
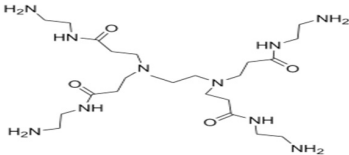
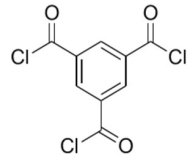
Amine	Chemical Structure	Acid Chloride	Chemical Structure	Membrane Performance	Ref.
MPD		TMC		It is well-known that the interfacial polymerization of MPD and TFC on a porous support layer results in high water flux and salt rejection	[17]
BDSA		TMC		Water Flux increased by more than 100% by using BDSA in the interfacial polymerization. Simultaneously, salt rejection increased from 89 to 99%.	[24]
S-BAPS		TMC		When compared to the traditional TFC membrane, this membrane showed higher water flux, but lower NaCl rejection and chlorine resistance.	[25]
BHDT		TMC		This membrane demonstrated higher chlorine resistance when compared to the normal TFC membrane.	[26]
PAMAM		TMC		In this study, the effects of PAMAM content on TFC membrane performance were studied. NaCl rejection was increased when PAMAM concentration was increased from 0.1% to 0.5% (w/v), while water flux was reduced.	[27]

Table 1. Cont.

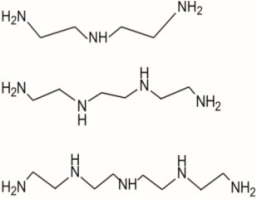
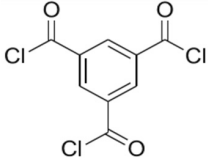
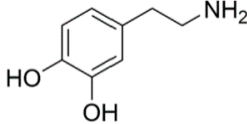
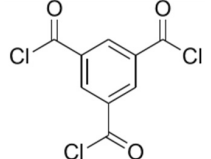
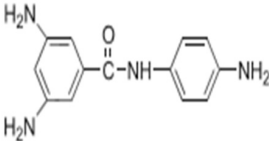
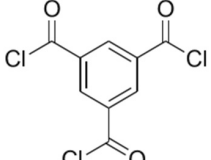
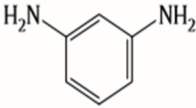
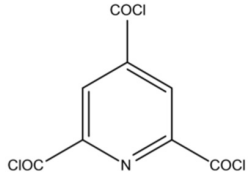
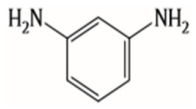
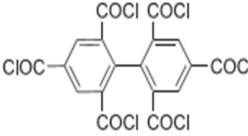
DETA, TETA, or TEPA	 <p>Chemical structures of DETA (diethylenetriamine), TETA (triethylenetriamine), and TEPA (tetraethylenetriamine).</p>	TMC	 <p>Chemical structure of TMC (trimellitic chloride).</p>	<p>Under operating pressure of 36.52 psi, water fluxes of TEPA/TMC, TETA/TMC, and DETA/TMC were 51.1 ± 4.5, 43.5 ± 0.5, and 33.5 ± 2 L/m²·h, respectively. On the other hand, Na₂SO₄ rejection sequence was: DETA/TMC > TEPA/TMC > TETA/TMC.</p>	[28]
DPA	 <p>Chemical structure of DPA (3-aminophenol).</p>	TMC	 <p>Chemical structure of TMC (trimellitic chloride).</p>	<p>The polyester bonds of DPA/TMC produced TFC membrane with high chemical stability, while maintaining good performance.</p>	[29]
DABA	 <p>Chemical structure of DABA (4,4'-diaminobenzophenone).</p>	TMC	 <p>Chemical structure of TMC (trimellitic chloride).</p>	<p>Results showed that as DABA concentration was increased, the membrane became more hydrophilic and as a result, high water flux (55.4 L/m²·h-250 psi) was achieved.</p>	[23]
MPD	 <p>Chemical structure of MPD (3,4-diaminobenzophenone).</p>	DMSO	 <p>Chemical structure of DMSO (dimethyl sulfoxide).</p>	<p>The developed membrane showed excellent antimicrobial efficiency and high water flux and salt rejection.</p>	[30]
MPD	 <p>Chemical structure of MPD (3,4-diaminobenzophenone).</p>	BTAC	 <p>Chemical structure of BTAC (benzophenone tetracarboxylic acid chloride).</p>	<p>Membrane surface was highly negatively charged, smooth, and very thin, which in turn produced high fouling resistance.</p>	[31]

Table 1. Cont.

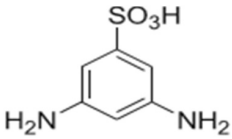
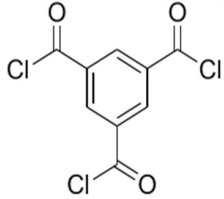
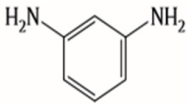
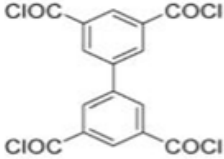
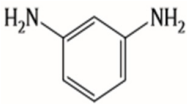
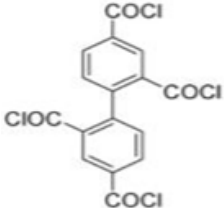
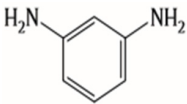
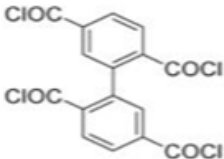
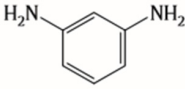
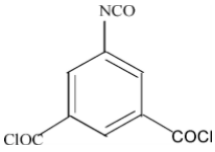
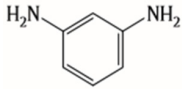
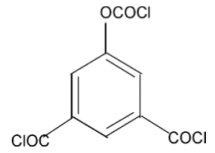
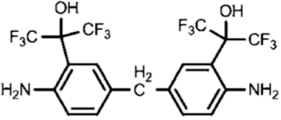
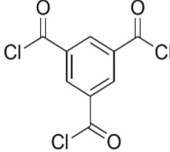
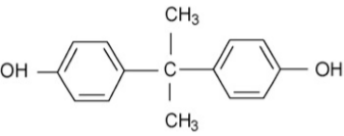
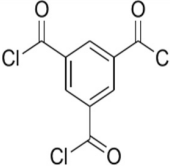
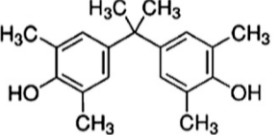
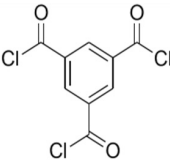
SMPD		TMC		When SMPS content was increased, the molecular weight of PA was decreased, and it subsequently increased water flux and decreased NaCl rejection.	[32]
MPD		mm-PETC		Under 290 psi, water flux was 37.1 L/m ² ·h and NaCl rejection was 98.4%	
MPD		om-PETC		Under 290 psi, water flux was 50 L/m ² ·h and NaCl rejection was 97.8%	[22]
MPD		op-PETC		Under 290 psi, water flux was 45.2 L/m ² ·h and NaCl rejection was 97.2%	

Table 1. Cont.

MPD		ICIC		Under operating pressure of 232 psi, water flux was 63 L/m ² ·h and NaCl rejection was 98.2%. In addition, the membrane showed significant resistance against chlorine.	[33]
MPD		CFIC		Under operating pressure of 232 psi, water flux was around 43.3 L/m ² ·h and NaCl rejection was around 98.6%. In addition, the membrane showed significant resistance against chlorine.	[33]
HFA-MDA		TMC		Under operating pressure of 400 psi, NaCl rejection was 85% at low pH 4, but increased to 96.1% at pH 10. Water flux was 48 L/m ² ·h and 80 L/m ² ·h at pH 4 and pH 10, respectively. Besides, the membrane showed significant chlorine resistance.	[34]
Bisphenol A		TMC		This membrane showed significant fouling resistance along with high water flux and salt rejection.	[35]
TMBPA		TMC		Under operating pressure of 130 psi, water flux was 66.7 L/m ² ·h and the membrane showed good antifouling properties.	[36]

One challenge facing RO TFC membrane durability is the degradation of the PA layer by chlorination [37]. Liu et al. [33] used three different polyacyl chlorides including 5-isocyanato-isophthaloyl chloride (ICIC), 5-chloroformyloxy-isophthaloyl chloride (CFIC), and TMC to prepare the TFC membrane with high chlorine tolerance. Results showed that the membrane prepared from MPD-CFIC and MPD-TMC possessed better chlorine stability when compared to MPD-ICIC membrane. It has been pointed out that the urea bond (NHCONH-) in MPD-ICIC could be easily attacked by chlorine. Recently, a composite membrane with high chlorine resistance has prepared through interfacial polymerization of hexafluoroalcohol (HFA)-aromatic diamine and trimesoyl chloride (TMC) [34]. The steric and electron withdrawing properties of HFA groups mitigated the probability of chlorine attack on the benzene rings or amide groups in the PA layer.

In term of fouling resistance, Hilal et al. [35,36] prepared composite membranes with improved antifouling properties by interfacial polymerization of bisphenol A (BPA) and trimesoyl chloride (TMC). This was attributed to the strong repulsion force between the negatively-charged bisphenol and organic foulants.

3. Modification of Membrane Surface

It was found that membrane performance is greatly affected by the treating steps that follow the synthesis process [38–42]. Chemical surface modifications are one of the promising post-treatment techniques that have been widely used to enhance TFC membrane surface properties. For example, Mickols and coworkers [43] used ethylenediamine and ethanolamine to increase membrane hydrophilicity. Their study showed that increasing the hydrogen bonding at the PA layer could enhance the interaction between water molecules and membrane surface, resulting in high water flux. Another study by Kuehne et al. [44] demonstrated that soaking the membrane in a solution containing glycerol promoted surface wettability and a 70% increase in water flux was obtained.

Wilf et al. [45] coated poly(vinyl alcohol) on TFC membrane surface to enhance fouling resistance and membrane durability. The modified membrane demonstrated better resistance against organic fouling when compared with the normal TFC membrane. Moreover, the membrane showed good permeability and long-term stability. The enhanced fouling resistance was ascribed to the lower rate of organics adsorption on the coated membrane. Coatings of poly(*N,N*-dimethylaminoethyl methacrylate) (PDMAEMA) have also exhibited enhanced chlorine resistance according to Kang et al. [46]. Additionally, Sakar et al. [47] used dendrimer-based coatings to reduce fouling effects. Recently, Ngo et al. [48] used redox initiated graft polymerization to coat TFC membrane with hydrophilic poly(acrylic acid). The coated membrane had lower roughness than the virgin one, and subsequently better fouling resistance and water flux was achieved.

Wu et al. [49,50] used gas plasma treatment to modify the TFC membrane. More carboxylic groups were introduced onto the surface by oxygen gaseous plasma treatment, which resulted in high water flux. On the other hand, argon plasma treatment improved chlorine resistance by introducing more amide groups onto the membrane surface. In addition, Lin et al. [51] demonstrated that the antifouling properties of the TFC membrane could be improved by using atmospheric gas plasma treatment. This kind of treatment created a polymeric brush at membrane surface which was capable of mitigating the attachment of organic foulant, Figure 2. However, plasma-induced grafting is a promising approach to produce a membrane with significant performance; however, it has not been thoroughly investigated and further research in this area is required.

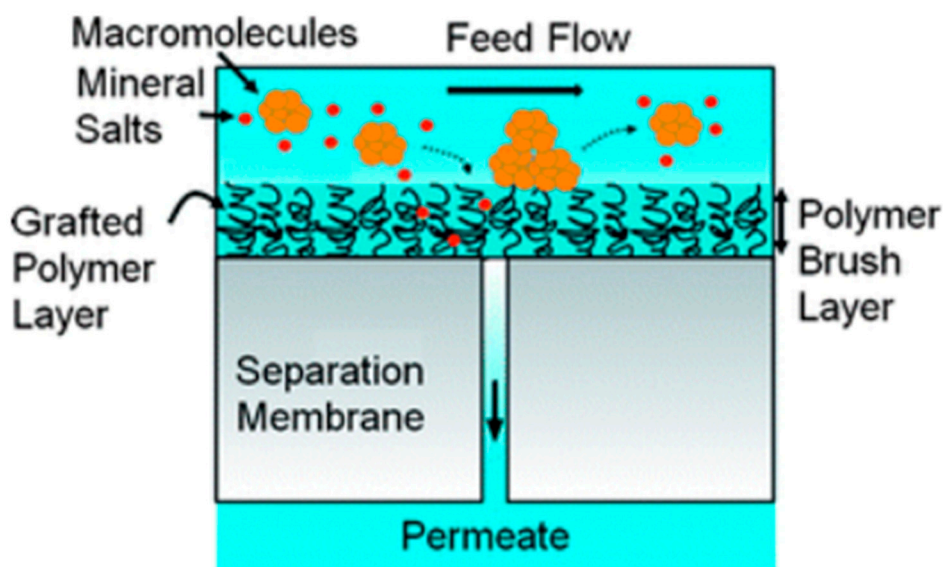


Figure 2. A schematic illustration of the nano-structured RO membrane, showing the antifouling polymeric brush, reproduced with permission from Lin et al. [51], with copyright permission from ©2010 Royal Society of Chemistry.

Bing et al. [52] used redox initiation to enhance TFC membrane performance, especially chlorine resistance. Immersing the membrane in potassium persulfate ($K_2S_2O_8$) solution initiated the interfacial crosslinking between the active film and PSU support, producing a thinner PA layer with more functional groups and denser cross linking. Reducing PA thickness led to enhanced water flux, as the water spent a shorter time to penetrate the membrane. On the other hand, increasing the crosslinking improved salt rejection by narrowing the passages for salt transportation. Moreover, the crosslinking reduced the N-chlorination sites on the membrane surface and hence, improved chlorine resistance.

4. Optimization of Polymerization Reactions

A major area of intense research is the optimization of interfacial polymerization reaction mechanisms such as kinetics, solvent solubility, reactant diffusion coefficient, reaction time, polymer molecular weight range, and characteristics of micro-porous support [53–56]. Tomaschke et al. [57] found that mixing amine salts with the casting solution formed a cross-linked membrane with an improved rejection. Chau et al. [58] added *N,N*-dimethyleformamide into a casting solution that introduced more carboxylic functional groups to PA layer, and eventually increased water flux. Kwak et al. [59] used dimethyl sulfoxide as an additive to modify the aromatic PA thin-film layer. The quantitative analysis of the surface morphology showed correlation between water permeability and both surface area and surface roughness; the flux improved with increasing roughness and surface area without a significant loss of salt rejection. Other researches showed that the addition of ethers, sulphur compounds, and alcohol- or water-soluble polymers to casting solution could produce high permeability without jeopardizing salt rejection [60–62].

Instead of modifying the casting solution, Michol et al. [63,64] succeeded in adding a complexing agent (phosphate containing compound) to the poly functional acyl halide prior to the substantial reaction between functional acyl halide and poly functional amide. It was thought that the addition of a complexing agent resulted in the formation of “association” with a polyfunctional acyl halide monomer capable of reducing the hydrolysis of acyl halide functional groups and permitting sufficient subsequent reaction with amine functional groups, thus resulting in a significant enhancement in membrane performance.

Another alternative approach for optimizing the polymerization reaction is to introduce surface-modified macromolecules (active additives) to acyl halide solution. This approach depends on the concept that the macromolecules may transfer to the PA film surface during the polymerization

and change surface properties of membrane whilst maintaining bulk properties unaltered [65,66]. Arafat et al. found that by using poly(ethylene glycol) as an active additive in the interfacial polymerization, the water flux and salt rejection were significantly increased [67].

5. Incorporation of Nanoparticles (NPs) into Membrane PA Layer

A new class of membrane has been formed by the incorporation of nanoparticles (NPs) into the top layer of conventional thin film composite membrane (fabrication process Figure 3). Table 2 summarized the performance of RO thin film nanocomposite (TFN) membranes that were reported in literatures and the next section discusses the most important studies.

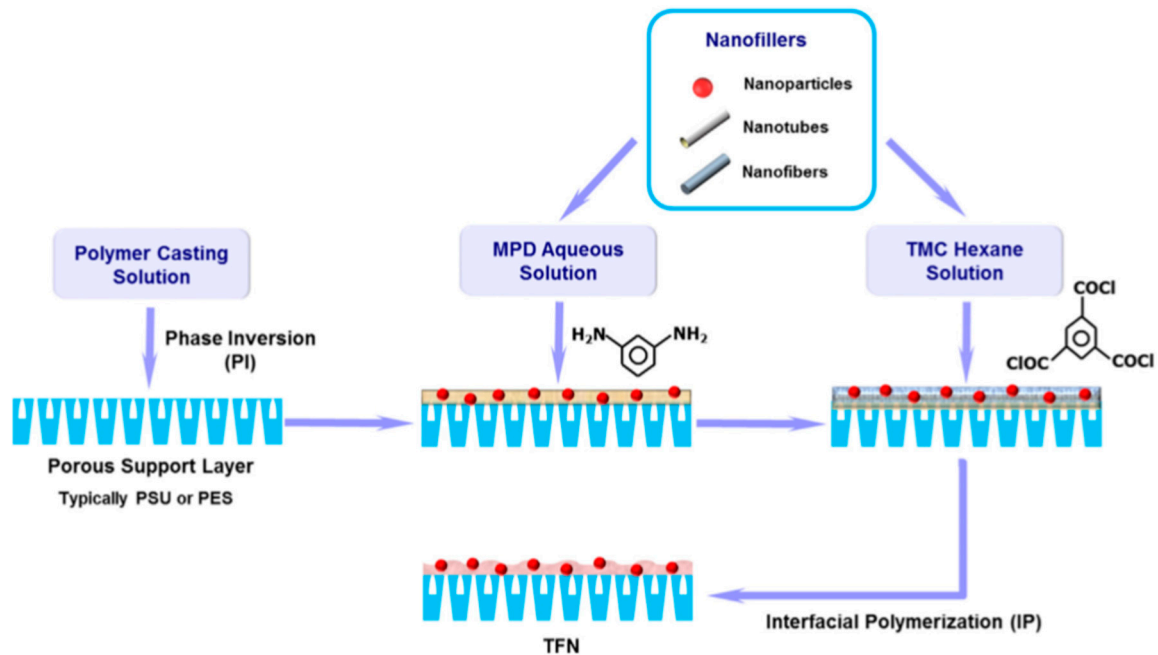


Figure 3. TFN membrane fabrication by the IP process, reproduced with permission from Yin et al. [19], with copyright permission from © 2014 Elsevier.

Table 2. Summary of important fillers used to modify TFC membranes.

Nanofiller	PA Layer Monomers	Substrate	Performance of TFN	Ref.
Zeolite NaA	MPD-TMC	PSU	Water flux was increased from 2.5×10^{12} to 3.9×10^{12} $\text{mPa}^{-1} \cdot \text{s}^{-1}$ without compromising salt rejection (94%) by increasing the concentration of nanoparticles from 0 to 0.4 wt. %.	[60]
Zeolite NaAAaA	MPD:TEA-TMC	PSU	Both AgA-TFN and NaA-TFN membranes exhibited higher water flux than that of TFC membrane. No change in salt rejection was observed. Both membranes showed enhanced antimicrobial properties.	[61]
Different sized zeolite	MPD:TEA:SLS:IPA-TMC	PSU	The membrane embedded with smaller zeolite NPs produced higher water flux than the membrane with larger zeolite NPs.	[62]
Silica	MPD-TMC	PSU	By increasing silica concentration, the thermal properties of the membrane were considerably enhanced.	[68]
MWCNTs	MPD-TMC	PSU	Under filtration pressure of 225 psi, both water flux and salt rejection were decreased from 18 to 12 $\text{L}/\text{m}^2 \cdot \text{h}$ and 98 to 92.2 wt.%, respectively, by increasing the concentration of MWCNTs from 0 to 1 wt.%. On the other hand, the membrane demonstrated significant chlorine resistance.	[69]
Zeolite -LTA	MPD-TMC-post Treatment	PSU	NaCl rejection and water flux were 99.4 wt.% and 42 $\text{L}/\text{m} \cdot \text{h}$, respectively, and had a filtration pressure of 300 psi.	[70]
F-Silica	MPD-TMC	PSU	When NPs concentration was 0.4 wt.%, the membrane showed high thermal stability.	[71]
F-MWCNTs	MPD-TMC	PSU	The membrane showed high dyes and brilliant blue rejection (91%)	[72]
Metal alkoxide	MPD: SLS-TMC	PSU	Water flux was increased by approximately 2-fold when compared with the virgin membrane.	[73]
Zeolite NaX	MPD-TMC	PES	Under filtration pressure of 175 psi, the water flux was increased from 8.01 to 29.76 $\text{L}/\text{m}^2 \cdot \text{h}$ by increasing the content of NPs from 0 to 0.2 wt.% without jeopardizing NaCl rejection (above 90%). Also, the membrane showed good thermal stability.	[74]
iLSMM	MPD-TMC	PSU	Under filtration pressure of 300 psi, the optimized water flux was 42 $\text{L}/\text{m}^2 \cdot \text{h}$ and the NaCl rejection was 97%. Besides, the membrane showed good antifouling properties.	[75]
MCM-41	MPD-TMC	PSU	Under filtration pressure of 300 psi, Water flux was increased from 28 to 46 $\text{L}/\text{m}^2 \cdot \text{h}$ by increasing the concentration of NPs from 0 to 0.1 wt.%, while NaCl rejection was maintained (97 wt.%).	[76]
APQZ	MPD-TMC	PSU	Water flux was increased from 16 to 40 $\text{L}/\text{m}^2 \cdot \text{h}$ by increasing the concentration of NP from 0 to 0.1 wt.%. In addition, the membrane showed good mechanical stability.	[77]

Table 2. Cont.

Zwitterion-CNT	MPD-TMC	PES	Under 530 psi, the optimized water flux was 48.46 L/m ² ·h, and NaCl rejection was 98.6%.	[78]
Carboxylic MWNTs	MPD-TMC	PES	Under 100 psi, the optimized water flux was 40 L/m ² ·h. Moreover, the membrane showed good mechanical stability.	[79]
Zeolite (Silicate-1)	MPD-TMC	PSU	The membrane showed higher chemical stability than the one with NaX-Zeolite NPs.	[80]
Zeolite-NaA	MPD-TMC	PSU	Under 232 psi, good water flux was achieved (46.5 L/m ² ·h) by adding the NPs in organic phase and high salt rejection (97%) by adding the NPs in aqueous phase.	[81]
Aminated Zeolite	MPD:aPES:TEA-TMC	PSU	Under 797 psi, adding PES and TEA to MPD-nanoparticle solution increased water flux from 23.2 to 37.8 L/m ² ·h without compromising salt rejection (98%). Moreover, the membrane showed good chlorine resistance.	[82]
Zeolite-A	MPD-TMC	PSU	The membrane showed significant fouling resistance.	[83]
Mesoporous SiO ₂	MPD-TMC	PSU	Under 232 psi, water flux was increased from 19 to 53 L/m ² ·h by increasing the concentration of NPs from 0 to 0.1 wt.%, while NaCl rejection remained (97%).	[84]
HBP-g-silica	MPD: aPES-TMC	PSU	Under 797.7 psi, the optimized water flux was 34.4 L/m ² ·h, while the salt rejection was 97.7%. And, the membrane showed better chlorine resistance.	[85]
Aluminosilicate CNTs	MPD-TMC	PSU	Under 232 psi, the optimized water flux was 23 L/m ² ·h, while NaCl rejection was 97.5%.	[86]
F-MWCNTs	MPD-TMC	PSU	Under 232 psi, the optimized water flux was 28.05 L/m ² ·h, while salt rejection was 90%. In addition, the membrane showed better antifouling and antioxidant properties.	[87]
HNTs	MPD-TMC	PSU	Under 217.5 psi, water flux was increased from 18 to 36.1 L/m ² ·h by increasing the concentration of NPs from 0 to 0.1% without sacrificing NaCl rejection (93%). Besides, the membrane had enhanced fouling properties.	[88]
OA-SiO ₂	MPD-TMC	PSU	The OA modified-silica PA membrane produced higher salt rejection (98%) when compared to the unmodified silica PA membrane (95%).	[89]
Clay	MPD-TMC	PSU	Under 232 psi, water flux was increased from 36.6 to 51 L/m ² ·h by adding 0.1 wt.% NPs without compromising NaCl rejection (around 99%). Also, the membrane exhibited significant antifouling properties.	[90]
GO-TiO ₂	MPD-TMC	PSU	Under 217.5 psi, both water flux and salt rejection were increased from 34 to 51 L/m ² ·h and 97 to 99%, respectively, by adding 0.02 wt.% NPs. Besides, the membrane demonstrated robust chlorine resistance.	[91]

Table 2. Cont.

HN ₂ -TNTs	MPD-TMC	PSU	Under 217.5 psi, both water flux and NaCl rejection were increased from 19 to 36 L/m ² ·h and 94 to 96%, respectively, by adding 0.05 wt.% NPs. Moreover, the membrane showed good fouling resistance.	[92]
GO	MPD-TMC	PSU	Under 217 psi, the optimized water flux was 22 L/m ² ·h, while NaCl rejection was above 80%. Moreover, the modified membrane exhibited excellent fouling resistance against BSA and HA.	[93]
Al-ZnO	MPD-TMC	PSU	Under 225 psi, the optimized water flux was 32 L/m ² ·h, while NaCl rejection was 98%.	[94]
MCM-48-SiO ₂	MPD-TMC	PSU	Under 232 psi, the optimized water flux was 68 L/m ² ·h. And, NaCl rejection was around 97%.	[95]
GO	MPD-TMC	PSU	Under 300 psi, water flux was increased from 39 to 60 L/m ² ·h by increasing NPs concentrations from 0 to 0.015 wt.%, while NaCl rejection was above 93%.	[96]
ZnO	MPD-TMC	PSU	Under 300 psi, water flux was increased from 60 to 85 L/m ² ·h by increasing the concentration of ZnO from 0 to 0.1 wt.%. Under UV irradiation the membrane showed super water flux (120 L/m ² ·h). In addition, the membrane showed excellent fouling resistance.	[97]
MOFs	MPD-TMC	PSU	Under operation pressure of 300 psi, water flux and NaCl rejection were 85 L/m ² ·h and 98.5%, respectively.	[98]
Graphene quantum dots	PIP-TMC	PES	Under operation pressure of 0.2 Mpa, water flux was 120 L/m ² ·h, 6.8-times higher than that of the virgin membrane. Moreover, the membrane showed excellent fouling resistance.	[99]
ZIF-8	MPD-TMC	PSU	53% enhancement in water flux was achieved. NaCl rejection was 99.4%.	[100]
TiO ₂	MPD-TMC	PES	The addition of TiO ₂ resulted in higher water flux (24.3 L/m ² ·h) as compared with the virgin TFC (21.5 L/m ² ·h), while membrane selectivity was preserved (97%). Additionally, by increasing feed solution temperature from 25 to 65 °C, further enhancement in water flux was achieved.	[101]
CQDs	PIP-TMC	PSU	The addition of carbon quantum dots led to significant increase in permeate flux (from 18 to 42.1 L/m ² ·h) without jeopardizing Na ₂ SO ₄ rejection (93%). Moreover, the fouling capacity of membrane was enhanced.	[102]
Na ⁺ functionalized CQDs	MPD-TMC	PES	Impressive water flux (104 L/m ² ·h), high rejection of SeO ₃ ²⁻ (97.5%), and excellent fouling resistance were achieved when quantum dots concentration was 0.05 wt.%.	[103]
SiO ₂	MPD-TMC	PSU	Water flux was increased from 30 to 50 L/m ² ·h by increasing NPs concentration from 0 to 0.1 wt.% along with slight increase in salt rejection (from 92 to 95%).	[104]
Zirconiumv (IV)-carboxylate MOFs	MPD-TMC	PSU-PVP-LiCl	52% increase in water flux was achieved without compromising NaCl rejection (95.5%).	[105]

Jeong and Huang [60] reported that adding NaA zeolite NPs into the PA could result in an increase in water permeability without decreasing salt rejection. It was claimed that the superior hydrophilicity, high negative surface charge, and internal pores of zeolite nanomaterial facilitated water absorption and movement across the membrane, while maintaining high salt rejection via Donnan exclusion.

Lind et al. [62] studied the influence of zeolite crystal size on the apparent structure, morphology, interface, and permeability of zeolite-PA TFN membranes. The existence of zeolite NPs resulted in higher permeability, greater negative surface charge, and thicker PA when compared with the raw membrane. The smaller NPs produced greater permeability, while the larger NPs produced more favorable surface properties. This study implied that the size of NPs may be considered an additional “degree of freedom” in designing the nanostructured membranes. Recently, Mayyahi [106] used quantum dots as an ultra-small filler to modify the TFN. Both water flux and salt rejection were increased upon the addition of QDs.

Another study by Fathizadeh et al. [74] showed that increasing MPD and TMC concentrations to 3% *w/v* and 0.15% *w/v*, respectively, during TFN preparation in the presence of zeolite NPs formed a membrane with superior water flux but declined NaCl rejection. The low solute rejection was attributed to the poor dispersion of nanoparticles in the high molecular weight PA layer. The aggregation of NPs could have generated micro-holes in the PA, which allowed the brackish water to pass through. The reported results suggested that the relation between NPs and IP condition is another important factor that needs to be addressed.

In addition to zeolite, different NPs such as nano-silica [68,71,104], multiwall carbon nanotubes [69,72], zwitterion functionalized-carbon nanotubes [78], Titanium dioxide (TiO₂) [101,107], and clay nano-sheets [90] have been used to modify the composite membranes. All these researches showed that imparting NPs to the PA could enhance membrane performance in terms of permeate flux, salt rejection, chlorine resistance, and antifouling properties. For instant, Barona et al. [86] found that incorporating aluminosilicate single-wall carbon nanotubes (SWNTs) into the membrane surface resulted in a significant increase in water flux without affecting salt rejection. The functional groups on SWCNTs secured excellent dispersion of fillers in the PA and, as a result, enhanced the overall performance. A remarkable enhancement in membrane performance was achieved in another study by Jun et al. [76] upon the addition of MCM-41 silica NPs without compromising salt rejection. The high water permeability was ascribed to the enhanced membrane hydrophilicity as well as the pores in the NPs that imparted extra channels for water transportation.

It is known that PA composite membranes are very sensitive to chlorine. As the PA layer touches the chlorinated water, the amine groups oxidize by chlorine and decompose in water, leading to deteriorated separation performance [108]. Park et al. [69] used acid functionalized MWCNTs to improve the chlorine resistance. When MWCNTs were incorporated into the PA active layer, the membrane showed enhanced anti-chlorine properties. This could be ascribed to the reaction between the functional groups in carbon nanotubes and the amine groups in PA structure, which as a result formed a barrier above the PA that reduced membrane chlorine exposure. Another study by Kim et al. [85] showed that attaching hyper branched polyamide modified silica NPs onto PA layer could protect the membrane from chlorine attack. The extra amino groups presented by the functionalized silica NPs were the main target for chlorine and subsequently lessened membrane surface exposure, as shown in Figure 4. It seems that all researchers followed the same strategy to produce a membrane with high chlorine resistance, which generates a protection layer on the membrane surface; however, this could not provide long term efficiency as the barrier might be finally degraded and the chlorine reaches the membrane surface [82,87,109].

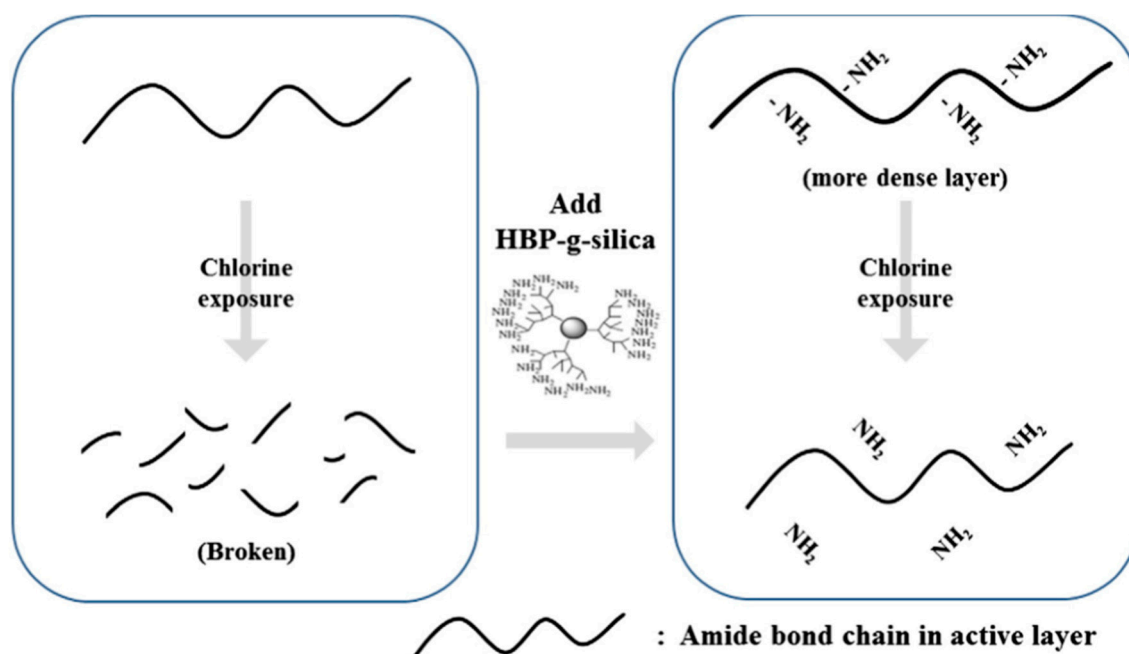


Figure 4. Protection sequence against chlorine attack, reproduced with permission from Kim et al. [85], with copyright permission from © 2013 Elsevier.

Membrane fouling is generally known as the accumulation of unwanted materials on membrane surfaces [110]. Organic and micro-biological fouling of TFN membranes are among the substantial reasons that lead to membrane performance decline [111]. Hence, many studies are devoted to develop a TFC with desired fouling resistance without “trading off” any of the other properties including permeability and rejection efficiency. Kim et al. [112] showed that incorporating hydrophilic filler into the PA layer could increase membrane resistance against organic fouling. The results demonstrated that there was a reverse relationship between hydrophilicity and organic foulants accumulation. This could be ascribed to the weak interaction between organic foulants and hydrophilic surfaces. Another study by Rana et al. [75] exhibited that an increase in membrane’s negative surface charge could enhance fouling resistance, due to the strong repulsive force between the membrane and negatively charged foulants. Lee et al. [113] used Ag nanoparticles as fillers in the PA to mitigate bacterial accumulation on the surface. Results showed that the Ag-TFN membrane has better resistance against bacterial fouling. It is believed that Ag nanoparticles disturb the permeability and respiration functions of the bacterial cell, and eventually destroy the DNA [114–116].

Kim et al. used a new approach to prepare hybrid TFC by the self-assembly between titanium oxide NPs and PA’s carboxylic functional groups [117]. Results indicated that the UV irradiation of the membrane could reduce E-coli content on the surface and this was attributed to the ability of TiO₂ to form different hydroxyl and peroxide radicals under the influence of UV light. These active radicals were capable of destroying the bacterial cells. Ben-Sasson et al. [116] used electrostatic attraction to attach copper (Cu) nanoparticles to the TFC membrane surface. Results indicated that the presence of positively charged Cu-NPs did not affect the overall hydrophilicity of the membrane, but reduced the growth of bacterial cells. The SEM images of the membrane’s surface exhibited that the bacterial cells were damaged when contacted with Cu-NPs. This could be ascribed to the high toxicity of Cu that led to bacterial DNA damage. Choi et al. [118] used “layer-by-layer assembly” to attach graphene oxide (GO) and aminated-graphene oxide (AGO) to TFC membrane surface, as shown in Figure 5. The resultant TFC showed enhanced resistance against organic fouling and chlorine attack, while preserving water flux and NaCl rejection. Hu and Mi [119] succeeded in using layer-by-layer deposition” to connect GO NPs to the PA. In this case, GO-NPs formed linkages with membrane’s

functional groups. The newly developed membrane exhibited superior water flux and excellent dye rejection. The disadvantage of the “surface located nanocomposite membrane” is the loss of nanoparticles during filtration, especially those attached by electrostatic forces. The depletion of nanoparticles reduces the efficiency of the membrane and may expose nanoparticles to the permeated water causing a threat to people’s health. As a result, Yin and co-workers. [120] used cysteamine as a “bridging agent” to attach silver (Ag) nanoparticles to the membrane surface, as shown in Figure 6. Results indicated that the modified membrane has stable Ag NPs, superior antimicrobial properties, high permeability, and good separation efficiency. Recently, Mayyahi [121] showed that UV irradiation of TFN membrane which impregnated with TiO₂ could result in robust antibacterial properties.

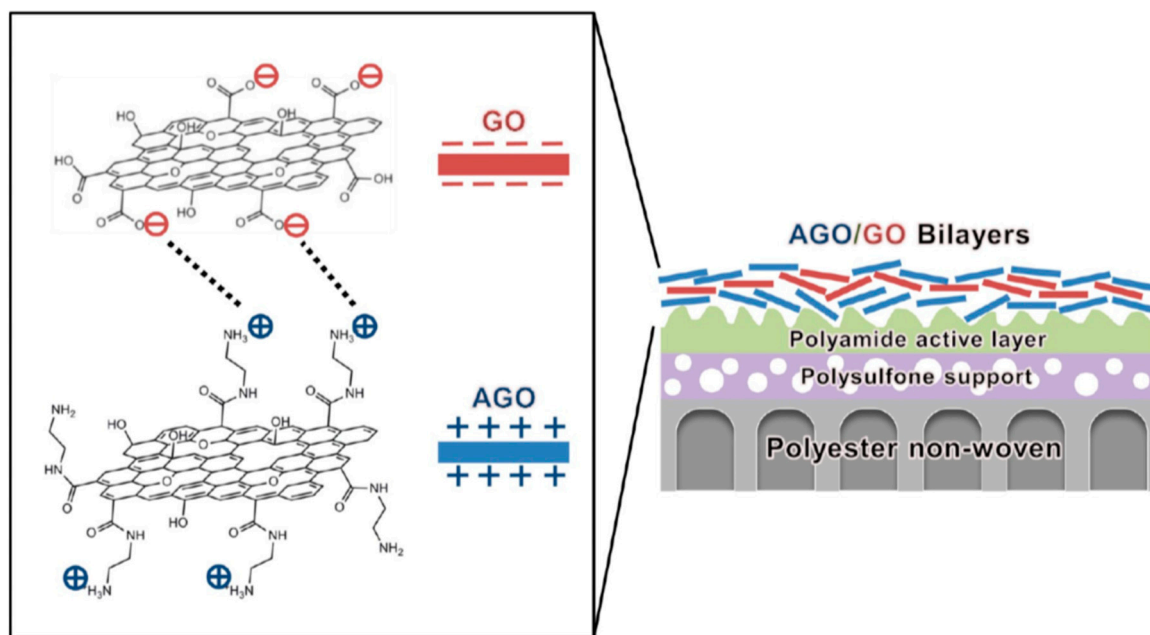


Figure 5. Layer-by-layer deposition of positively-charged GO and aminated-GO nanosheets on the membrane surface; reproduced with permission from Choi et al. [118], with copyright permission from © 2013, American Chemical Society.

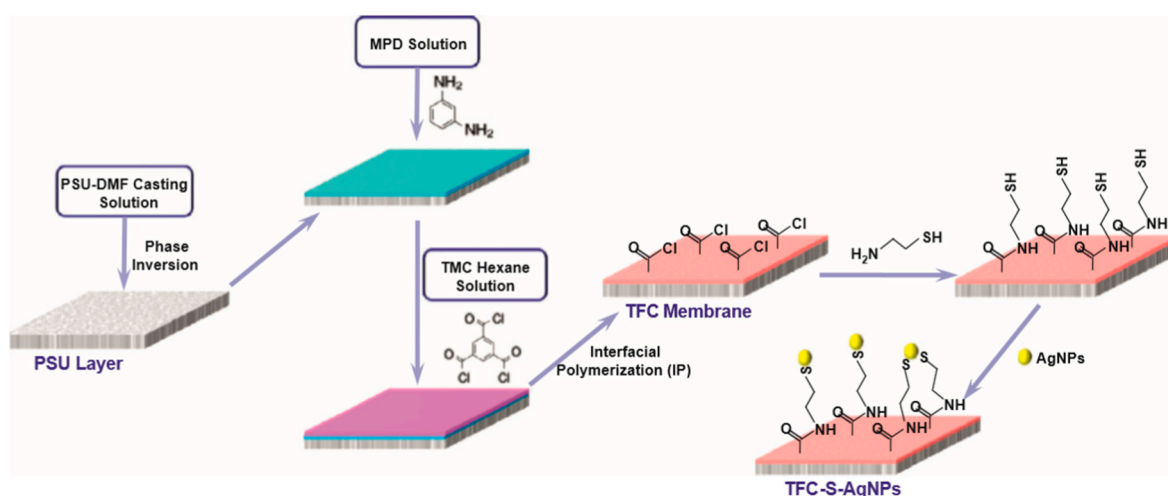


Figure 6. Schematic illustration of attaching Ag-NPs on the TFC membrane surface; reproduced with permission from Yin et al. [120], with copyright permission from © 2013 Elsevier.

6. Conclusions

A tremendous development in TFN membranes for water purification has been achieved including producing a membrane with super water flux, high salt rejection, and excellent fouling and chlorine resistance via using innovative approaches such as imparting the favored properties of nanoparticles to the membrane surface, optimizing the membrane fabrication process, modifying the materials that are required to synthesis the membrane, and changing membrane surface properties by post-treatment. However, researchers have failed to find an alternative to the PA barrier layer or to suggest a new support layer. We do agree that PA atop PSU/PES showed robust efficiency in RO and other water treatments applications, but these membranes have been used since 1970 and scholars have successfully addressed almost all the challenges facing the progress of such membranes. Forthcoming researches should be dedicated to suggest a new reverse osmosis membrane rather than developing the existing one.

Funding: This research received no external funding.

Conflicts of Interest: The author declares no conflict of interest.

Abbreviations

AGO	Aminated-graphene oxide
Ag	Silver
Al-ZnO	Aluminum doped zinc oxide
BDSA	2,2'-benzidinedisulfonic acid
BHAC	2,2',4,4',6,6'-biphenyl hexaacyl chloride
BHDT	Bis-2,6- <i>N,N</i> -(2-hydroxyethyl) diaminotoluene
BPA	Bisphenol
CFIC	5-chloroformyloxy-isophthaloyl chloride
CNT	Carbon nanotube
CQDs	Carbon quantum dots
Cu	Copper
DABA	Triamine 3,5-diamino- <i>N</i> -(4-aminophenyl)-benzamide
DMF	<i>N,N</i> -dimethylformamide
DMSO	2,4,6-pyridinetricarboxylic acid chloride
DETA	Diethylenetriamine
DPA	Dopamine
F-MWCNTs	Functionalized multi wall carbon nanotubes
F-silica	Functionalized silica
GO	Graphene oxide
HBP-g-silica	Hyper-branched aromatic polyamide-grafted silica
HNTs	Halloysite nanotubes
ICIC	5-isocyanato-isophthaloyl chloride
IP	Interfacial polymerization
iLSMM	In-situ hydrophilic surface modifying macromolecules
MOFs	Metal-organic frameworks
MPD	<i>m</i> -phenylenediamine
mm-BTEC	3,3',5,5'-biphenyl tetraacyl chloride
MWCNTs	Multiwall carbon nanotubes
NPs	Nanoparticles
OA-SiO ₂	Oleic acid modified silica
om-BTEC	2,2',4,4'-biphenyl tetraacyl chloride
MOFs	Metal-organic framework
op-BTEC	2,2',5,5'-biphenyl tetraacyl chloride
PA	Polyamide
PAMAM	Ethylenediamine cored poly(amidoamine)

PDMAEMA	Poly(<i>N,N</i> -dimethylaminoethyl methacrylate)
PSU	Polysulfone
RO	Reverse osmosis
SiO ₂	Silicon dioxide
SMPD	Sulfonated m-phenylenediamine
SWCNTs	Single-wall carbon nanotubes
TFC	Thin film composite
TFN	Thin film nanocomposite
TiO ₂	Titanium dioxide
TMC	Trimesoyl chloride
TETA	Triethylenetetramine
TEPA	Tetraethylenepentamine
TNTs	Titanate nanotubes
UV	Ultraviolet
ZIF	Zeolitic imidazolate framework
ZnO	Zinc oxide

References

- Marry, P.; Hoek, E. A review of water treatment membrane nanotechnologies. *Energy Environ. Sci.* **2011**, *4*, 1946–1971.
- Elimelech, M.; Phillip, W.A. The future of seawater desalination: energy, technology, and the environment. *Science* **2011**, *333*, 712–717. [[CrossRef](#)] [[PubMed](#)]
- Li, N.; Fane, A.; Hu, W.; Matsuura, T. *Advanced Membrane Technology and Applications*; John Wiley & Sons: Hoboken, NJ, USA, 2008.
- Shenvi, S.; Isloor, A.; Ismail, A. A review on RO membrane technology: Developments and challenges. *Desalination* **2015**, *368*, 10–26. [[CrossRef](#)]
- Malaeb, L.; Ayoub, G. Reverse osmosis technology for water treatment: State of the art review. *Desalination* **2011**, *267*, 1–8. [[CrossRef](#)]
- Mai, Z. Membrane Processes for Water and Wastewater Treatment: Study and Modeling of Interactions between Membrane and Organic Matter. Ph.D. Thesis, LGPM—Laboratoire de Génie des Procédés et Matériaux, Paris, France, 2013.
- Wijmans, J.G.; Baker, R.W. The solution-diffusion model: A review. *J. Membr. Sci.* **1995**, *107*, 1–21. [[CrossRef](#)]
- Soltanieh, M.; Gill, W.N. Review of reverse osmosis membrane and transport models. *Chem. Eng. Commun.* **1981**, *12*, 279–363. [[CrossRef](#)]
- Lee, C.H. Theory of reverse osmosis and some other membrane permeation operations. *J. Appl. Polym. Sci.* **1975**, *19*, 83–95. [[CrossRef](#)]
- Reid, C.E.; Breton, E.J. Water and ion flow across cellulosic membranes. *J. Appl. Polym. Sci.* **1959**, *1*, 133–143. [[CrossRef](#)]
- Sourirajan, S. Separation of hydrocarbon liquids by flow under pressure through porous membranes. *Nature* **1964**, *203*, 1348–1349. [[CrossRef](#)]
- Loeb, S. *Sea Water Demineralization by Means of a Semipermeable Membrane: Progress Report July 1, 1962–December 31*; University of California: Berkeley, CA, USA, 1963.
- Porter, M.C. What, when and why of membranes MF, UF, and RO. *ALChESymp. Ser.* **1977**, *73*, 83–103.
- Burns and Roe Industrial Services Corporation. *Reverse Osmosis Technical Manual*; United States Office of Water Research and Technology: Washington, DC, USA, 1979.
- Belfort, G. Chapter 6: Pressure driven membrane processes and wastewater renovation in water renovation and reuse. In *Water Renovation and Reuse*, 1st ed.; Shuval, H., Ed.; Academic Press: Cambridge, MA, USA, 1977.
- Shields, C.P. Five years' experience with reverse osmosis systems using DU PONT "Permasp" permeators. *Desalination* **1979**, *28*, 157–179. [[CrossRef](#)]
- Cadotte, J.E. Interfacially Synthesized Reverse Osmosis Membrane. U.S. Patent 4,277,344, 7 July 1979.
- Khorshidi, B.; Thundat, T.; Fleck, B.A.; Sadrzadeh, M. A novel approach toward fabrication of high performance thin film composite polyamide membranes. *Sci. Rep.* **2016**, *6*, 22029. [[CrossRef](#)] [[PubMed](#)]

19. Yin, J.; Deng, B. Polymer-matrix nanocomposite membranes for water treatment. *J. Membr. Sci.* **2015**, *479*, 256–275. [[CrossRef](#)]
20. Xu, G.R.; Xu, J.M.; Feng, H.J.; Zhao, H.L.; Wu, S.B. Tailoring structures and performance of polyamide thin film composite (PA-TFC) desalination membranes via sublayers adjustment—A review. *Desalination* **2017**, *417*, 19–35. [[CrossRef](#)]
21. Gohil, J.M.; Ray, P. A review on semi-aromatic polyamide TFC membranes prepared by interfacial polymerization: Potential for water treatment and desalination. *Sep. Purif. Technol.* **2017**, *181*, 159–182. [[CrossRef](#)]
22. Li, L.; Zhang, S.; Zhang, X.; Zheng, G. Polyamide thin film composite membranes prepared from isomeric biphenyl tetraacyl chloride and m-phenylenediamine. *J. Membr. Sci.* **2008**, *315*, 20–27. [[CrossRef](#)]
23. Wang, H.; Li, L.; Zhang, X.; Zhang, S. Polyamide thin-film composite membranes prepared from a novel triamine 3,5-diamino-N-(4-aminophenyl)-benzamide monomer and m-phenylenediamin. *J. Membr. Sci.* **2010**, *353*, 78–84. [[CrossRef](#)]
24. Nathaniel, G.; Lim, J.; Jung, B. High performance thin film composite polyamide reverse osmosis membrane prepared via m-phenylenediamine and 2,2-benzidinedisulfonic acid. *Desalination* **2012**, *291*, 69–77.
25. Xie, W.; Geise, G.; Freeman, B.; Lee, H.; Byun, G.; McGrath, J. Polyamide interfacial composite membranes prepared from m-phenylene diamine, trimesoyl chloride and a new disulfonated diamine. *J. Membr. Sci.* **2012**, *404*, 152–161. [[CrossRef](#)]
26. Zhang, Z.; Wang, S.; Chen, H.; Wang, T. Preparation of polyamide membranes with improved chlorine resistance by bis-2,6-N,N-(2-hydroxyethyl) diaminotoluene and trimesoyl chloride. *Desalination* **2013**, *331*, 16–25. [[CrossRef](#)]
27. Sum, J.Y.; Ahmad, A.; Ooi, B.S. Synthesis of thin film composite membrane using mixed dendritic poly(amidoamine) and void filling piperazine monomers. *J. Membr. Sci.* **2014**, *466*, 183–191. [[CrossRef](#)]
28. Li, Y.; Su, Y.; Dong, Y.; Zhao, X.; Jiang, Z.; Zhang, R.; Zhao, J. Separation performance of thin-film composite nanofiltration membrane through interfacial polymerization using different amine monomers. *Desalination* **2014**, *333*, 59–65. [[CrossRef](#)]
29. Zhao, J.; Su, Y.; He, X.; Zhao, X.; Li, Y.; Zhang, R.; Jiang, Z. Dopamine composite nanofiltration membranes prepared by self-polymerization and interfacial polymerization. *J. Membr. Sci.* **2014**, *465*, 41–48. [[CrossRef](#)]
30. Jewrajka, S.; Reddy, A.V.R.; Rana, H.; Mandal, S.; Khullar, S.; Haldar, S.; Joshi, N.; Ghosh, P. Use of 2,4,6-pyridinetri-carboxylic acid chloride as a novel co-monomer for the preparation of thin film composite polyamide membrane with improved bacterial resistance. *J. Membr. Sci.* **2013**, *439*, 87–95. [[CrossRef](#)]
31. Wang, T.; Dai, L.; Zhang, Q.; Li, A.; Zhang, S. Effects of acyl chloride monomer functionality on the properties of polyamide reverse osmosis (RO) membrane. *J. Membr. Sci.* **2013**, *440*, 48–57. [[CrossRef](#)]
32. Yong, Z.; Sanchuan, Y.; Meihong, L.; Congjie, G. Polyamide thin film composite membrane prepared from m-phenylenediamine and m-pheneylenediamine-5-sulfonic acid. *J. Membr. Sci.* **2006**, *270*, 162–168. [[CrossRef](#)]
33. Liu, M.; Wu, D.; Yu, S.; Gao, C. Influence of the polyacyl chloride structure on the reverse osmosis performance, surface properties and chlorine stability of the thin-film composite polyamide membranes. *J. Membr. Sci.* **2009**, *326*, 205–214. [[CrossRef](#)]
34. La, Y.; Sooriyakum, R.; Miller, D.; Fujiwara, M.; Freeman, B.; Allen, R. Novel thin film composite membrane containing ionizable hydrophobes: pH-dependent reverse osmosis behavior and improved chlorine resistance. *J. Mater. Chem.* **2010**, *20*, 4615–4620. [[CrossRef](#)]
35. Abu Seman, M.; Khayet, M.; Hilal, N. Nanofiltration thin-film composite polyester polyethersulfone-based membranes prepared by interfacial polymerization. *J. Membr. Sci.* **2010**, *348*, 109–116. [[CrossRef](#)]
36. Abu Seman, M.; Khayet, M.; Hilal, N. Development of antifouling properties and performance of nanofiltration membranes modified by interfacial polymerization. *Desalination* **2011**, *273*, 36–47. [[CrossRef](#)]
37. Koo, J.; Petersen, R.; Cadotte, J. ESCA characterization of chlorine-damage polyamide reverse osmosis membrane. *ACS Polym. Prepr.* **1986**, *27*, 391–392.
38. Liu, M.; Zhou, C.; Dong, B.; Wu, Z.; Wang, L.; Yu, S.; Gao, C. Enhancing the permselectivity of thin-film composite poly(vinyl alcohol) (PVA) nanofiltration membrane by incorporating poly(sodium-p-styrene-sulfonate) (PSSNa). *J. Membr. Sci.* **2014**, *463*, 173–182. [[CrossRef](#)]
39. Schafer, A.L.; Fane, A.G.; Waite, T.D. *Nanofiltration: Principles and Application*, 1st ed.; Elsevier: New York, NY, USA, 2003.

40. Petersen, R.J. Composite reverse osmosis and nanofiltration membrane. *J. Membr. Sci.* **1993**, *38*, 81–150. [[CrossRef](#)]
41. Hilal, N.; Al-Zoubi, H.; Darwish, N.A.; Mohamma, A.W.; Arabi, M.A. A comprehensive review of nanofiltration membranes: Treatment, pretreatment, modeling and atomic force microscopy. *Desalination* **2004**, *170*, 281–308. [[CrossRef](#)]
42. Lau, W.J.; Ismail, A.F. Polymeric nanofiltration membrane for textile dyeing waste treatment: preparation, performance evaluation, transport modeling, and fouling control—A review. *Desalination* **2010**, *245*, 4551–4566.
43. Mickols, W.E. Method of Treating Polyamide Membranes to Increase Flux. U.S. Patent 5,755,964, 26 May 1998.
44. Kuehne, M.A.; Song, R.Q.; Li, N.N.; Petersen, R.J. Flux enhancement in TFC RO membranes. *Environ. Prog.* **2001**, *20*, 23–26. [[CrossRef](#)]
45. Wilf, M.; Alt, S. Application of low fouling RO membrane elements for reclamation of municipal wastewater. *Desalination* **2000**, *132*, 11–19. [[CrossRef](#)]
46. Kang, G.D.; Gao, C.J.; Chen, W.D.; Jie, X.M.; Cao, Y.M. Study on hypochlorite degradation of aromatic polyamide reverse osmosis membrane. *J. Membr. Sci.* **2007**, *300*, 165–171. [[CrossRef](#)]
47. Sarkar, A.; Carver, P.I.; Zhang, T.; Merrington, A.; Bruza, K.J.; Rousseau, J.L.; Keinath, S.E.; Dvornic, P.R. Dendrimer-based coatings for surface modification of polyamide reverse osmosis membranes. *J. Membr. Sci.* **2010**, *349*, 165–171. [[CrossRef](#)]
48. Hong Anh Ngo, T.; Dinh Do, K.; Thi Tran, D. Surface modification of polyamide TFC membranes via redox-initiated graft polymerization of acrylic acid. *J. Appl. Polym. Sci.* **2017**, *134*, 45110. [[CrossRef](#)]
49. Wu, S.; Xing, J.; Zheng, C.; Xu, G.; Zheng, G.; Xu, J. Plasma modification of aromatic polyamide reverse osmosis composite membrane surface. *J. Appl. Polym. Sci.* **1997**, *764*, 1923–1926. [[CrossRef](#)]
50. Gilman, A.B. Low temperature plasma treatment as an effective method for surface modification of polymeric materials. *High Energy Chem.* **2003**, *37*, 17–23. [[CrossRef](#)]
51. Lin, N.H.; Kim, M.M.; Lewis, G.T.; Cohen, Y. Polymer surface nano-structuring of reverse osmosis membrane for fouling resistance and improved flux performance. *J. Membr. Sci.* **2010**, *20*, 4642–4652. [[CrossRef](#)]
52. Bing, S.; Wang, J.; Xu, H.; Zhao, Y.; Zhou, Y.; Zhang, L.; Gao, C.; Hou, L.A. Polyamide thin-film composite membrane modified with persulfate for improvement of perm-selectivity and chlorine-resistance. *J. Membr. Sci.* **2018**, *555*, 318–326. [[CrossRef](#)]
53. Song, Y.; Sun, P.; Henry, L.L.; Sun, B. Mechanism of structure and performance controlled thin film composite membrane formation via interfacial polymerization process. *J. Membr. Sci.* **2005**, *251*, 67–79. [[CrossRef](#)]
54. Karode, S.K.; Kulkarni, S.S.; Suresh, A.K.; Mashelkar, R.A. New insight into kinetics and thermodynamics of interfacial polymerization. *Chem. Eng. Sci.* **1998**, *53*, 2649–2663. [[CrossRef](#)]
55. Dhumal, S.S.; Wagh, S.J.; Suresh, A.K. Interfacial polymerization-modeling of kinetics and film properties. *J. Membr. Sci.* **2008**, *352*, 758–771. [[CrossRef](#)]
56. Ghosh, A.K.; Hoek, E.M.V. Impact of reaction and curing condition on polyamide composite reverse osmosis membrane properties. *J. Membr. Sci.* **2008**, *311*, 34–45. [[CrossRef](#)]
57. Tomaschke, J.E. Interfacially Synthesized Reverse Osmosis Membrane Containing an Amine Salt and Processes for Preparing the Same. U.S. Patent 4,948,507, 14 August 1990.
58. Chau, M.M.; Light, W.G.; Chu, H.C. Dry High Flux Semipermeable Membrane. U.S. Patent 4,983,291, 18 January 1991.
59. Kwak, S.Y.; Jung, S.G.; Kim, S.H. Structure-motion-performance relationship of flux enhanced reverse osmosis (RO) membranes composed of aromatic polyamide thin films. *Environ. Sci. Technol.* **2001**, *35*, 4334–4340. [[CrossRef](#)] [[PubMed](#)]
60. Jeong, B.-H.; Hoek, E.M.V.; Yan, Y.; Subramani, A.; Huang, X.; Hurwitz, G.; Ghosh, A.K.; Jawor, A. Interfacial polymerization of thin film nanocomposites: A new concept for reverse osmosis membranes. *J. Membr. Sci.* **2007**, *294*, 1–7. [[CrossRef](#)]
61. Lind, M.L.; Jeong, B.H.; Subramani, A.; Huang, X.; Hoek, E.M.V. Effect of mobile cation on zeolite-polyamide thin film nanocomposite membranes. *J. Mater. Res.* **2009**, *24*, 1624–1631. [[CrossRef](#)]
62. Lind, M.L.; Ghosh, A.K.; Jawor, A.; Huang, X.; Hou, W.; Yang, Y.; Hoek, E.M.V. Influence of zeolite crystal size on zeolite-polyamide thin film nanocomposite membranes. *Langmuir* **2009**, *25*, 10139–10145. [[CrossRef](#)] [[PubMed](#)]
63. Mickols, W.E. Composite Membrane and Method for Making the Same. U.S. Patent 6,878,278, 12 April 2005.

64. Mickols, W.E. Composite Membrane and Method for Making the Same. U.S. Patent 6,337,018, 8 January 2002.
65. Khayet, M. Membrane surface modification and characterization by X-ray Photo electron spectroscopy, atomic force microscopy and contact angle measurement. *Appl. Surf. Sci.* **2004**, *238*, 269–272. [[CrossRef](#)]
66. Khayet, M.; Suk, D.E.; Narbaitz, R.M.; Santerre, J.P. study on surface modification by surface modifying macromolecules and its application in membrane separation process. *Appl. Polym.* **2003**, *89*, 2902–2961. [[CrossRef](#)]
67. Tarboush, B.J.A.; Ranan, D.; Matsuura, T.; Nabratiz, H.A. Preparation of thin film composite polyamide membrane for water desalination using novel hydrophilic surface modifying macromolecules. *J. Membr. Sci.* **2008**, *325*, 166–175. [[CrossRef](#)]
68. Jadav, G.L.; Singh, P.S. Synthesis of novel silica-polyamide nanocomposite membrane with enhanced properties. *J. Membr. Sci.* **2009**, *328*, 257–267. [[CrossRef](#)]
69. Park, J.; Choi, W.; Kim, S.H.; Chun, B.H.; Bang, J.; Lee, K.B. Enhancement of chlorine resistance in carbon nanotube-based nanocomposite reverse osmosis membranes. *Desalin. Water Treat.* **2010**, *15*, 198–204. [[CrossRef](#)]
70. Lind, M.L.; Suk, D.E.; Nguyen, T.V.; Hoek, E.M.V. Tailoring the structure of thin film nanocomposite membranes to achieve seawater RO membrane performance. *Environ. Sci. Technol.* **2010**, *44*, 8230–8235. [[CrossRef](#)] [[PubMed](#)]
71. Jadav, G.L.; Aswal, V.K.; Singh, P.S. SANS study to probe nanoparticle dispersion in nanocomposite membranes of aromatic polyamide and functionalized silica nanoparticles. *J. Colloid. Interface Sci.* **2010**, *351*, 304–314. [[CrossRef](#)] [[PubMed](#)]
72. Roy, S.; Ntim, S.A.; Mitra, S.; Sirkar, K.K. Facile fabrication of superior nanofiltration membranes from interfacially polymerized CNT-polymer composites. *J. Membr. Sci.* **2011**, *375*, 81–87. [[CrossRef](#)]
73. Kong, C.; Koushima, A.; Kamada, T.; Shintani, T.; Kanezashi, M.; Yoshioka, T.; Tsuru, T. Enhanced performance of inorganic-polyamide nanocomposite membranes prepared by metal-alkoxide-assisted interfacial polymerization. *J. Membr. Sci.* **2011**, *366*, 382–388. [[CrossRef](#)]
74. Fathizadeh, M.; Aroujalian, A.; Raisi, A. Effect of added NaX nano-zeolite into polyamide as a top thin layer of membrane on water flux and salt rejection in a reverse osmosis process. *J. Membr. Sci.* **2011**, *375*, 88–95. [[CrossRef](#)]
75. Rana, D.; Kim, Y.; Matsuura, T.; Ararat, H.A. Development of antifouling thin film-composite membranes for seawater desalination. *J. Membr. Sci.* **2011**, *367*, 110–118. [[CrossRef](#)]
76. Yin, J.; Kim, E.S.; Yang, J.; Deng, B. Fabrication of a novel thin-film nanocomposite (TFN) membrane containing MCM-41 silica nanoparticles (NPs) for water purification. *J. Membr. Sci.* **2012**, *423*, 238–246. [[CrossRef](#)]
77. Zhao, Y.; Qiu, C.; Li, X.; Vararattanavech, A.; Shen, W.; Torres, J.; Hélix-Nielsen, C.; Wang, R.; Hu, X.; Fane, A.G.; et al. Synthesis of robust and high performance aquaporin-based biomimetic membranes by interfacial polymerization-membrane preparation and RO performance characterization. *J. Membr. Sci.* **2012**, *423*, 422–428. [[CrossRef](#)]
78. Chan, W.F.; Chen, H.Y.; Surapathi, A.; Taylor, M.G.; Shao, X.; Marand, E.; Johnson, J.K. Zwitterion functionalized carbon nanotube/polyamide nanocomposite membranes for water desalination. *ACS Nano* **2013**, *7*, 5308–5319. [[CrossRef](#)] [[PubMed](#)]
79. De Lannoy, C.F.; Jassby, D.; Gloe, K.; Gordon, A.D.; Wiesner, M.R. Aquatic biofouling prevention by electrically charged nanocomposite polymer thin film membranes. *Environ. Sci. Technol.* **2013**, *47*, 2760–2768. [[CrossRef](#)] [[PubMed](#)]
80. Huang, H.; Qu, X.; Ji, X.; Gao, X.; Zhang, L.; Chen, H.; Hou, L. Acid and multivalent ion resistance of thin film nanocomposite RO membranes loaded with silicalite-1 nanozeolites. *J. Mater. Chem. A* **2013**, *1*, 11343–11349. [[CrossRef](#)]
81. Huang, H.; Qu, X.; Dong, H.; Zhang, L.; Chen, H. Role of NaA zeolites in the interfacial polymerization process towards a polyamide nanocomposite reverse osmosis membrane. *RSC Adv.* **2013**, *3*, 8203–8207. [[CrossRef](#)]
82. Kim, S.G.; Hyeon, D.H.; Chun, J.H.; Chun, B.H.; Kim, S.H. Nanocomposite poly (arylene ether sulfone) reverse osmosis membrane containing functional zeolite nanoparticles for seawater desalination. *J. Membr. Sci.* **2013**, *443*, 10–18. [[CrossRef](#)]

83. Pendergast, M.M.; Ghosh, A.K.; Hoek, E.M.V. Separation performance and interfacial properties of nanocomposite reverse osmosis membranes. *Desalination* **2013**, *308*, 180–185. [[CrossRef](#)]
84. Bao, M.; Zhu, G.; Wang, L.; Wang, M.; Gao, C. Preparation of monodispersed spherical mesoporous nanosilica-polyamide thin film composite reverse osmosis membranes via interfacial polymerization. *Desalination* **2013**, *309*, 261–266. [[CrossRef](#)]
85. Kim, S.G.; Chun, J.H.; Chun, B.H.; Kim, S.H. Preparation, characterization and performance of poly(ethylene sulfone)/modified silica nanocomposite reverse osmosis membrane for seawater desalination. *Desalination* **2013**, *325*, 76–83. [[CrossRef](#)]
86. Baroña, G.N.B.; Lim, J.; Choi, M.; Jung, B. Interfacial polymerization of polyamide-aluminosilicate SWNT nanocomposite membranes for reverse osmosis. *Desalination* **2013**, *325*, 138–147. [[CrossRef](#)]
87. Zhao, H.; Qiu, S.; Wu, L.; Zhang, L.; Chen, H.; Cao, C. Improving the performance of polyamide reverse osmosis membrane by incorporating of modified multi wall carbon nanotubes. *J. Membr. Sci.* **2014**, *450*, 249–256. [[CrossRef](#)]
88. Ghanbaria, M.; Emadzadeh, D.; Lau, W.J.; Matsuura, T.; Ismail, A.F. Synthesis and characterization of novel thin film nanocomposite reverse osmosis membranes with improved organic fouling properties for water desalination. *RSC Adv.* **2015**, *5*, 21268–21276. [[CrossRef](#)]
89. Rakhshan, N.; Pakizeh, M. The effect of chemical modification of SiO₂ nanoparticles on the nanofiltration characteristics of polyamide membrane. *J. Membr. Sci.* **2015**, *32*, 2524–2533. [[CrossRef](#)]
90. Dong, H.; Wu, L.; Zhang, L.; Chen, H.; Cao, C. Clay nano-sheet as charged filler materials for highperformance and fouling resistance thin film nanocomposite membrane. *J. Membr. Sci.* **2015**, *494*, 92–103. [[CrossRef](#)]
91. Safarpour, M.; Khataee, A.; Vatanpour, V. Thin film nanocomposite reverse osmosis membrane modified by reduced graphene oxide/ TiO₂ with improved desalination performance. *J. Membr. Sci.* **2015**, *489*, 43–54. [[CrossRef](#)]
92. Emadzadeh, D.; Lau, W.J.; Rahbara, R.; Danseshfar, A.; Mayahi, A.; Matsuura, T.; Ismail, A.F. A novel thin film nanocomposite reverse osmosis membrane with superior anti organic fouling affinity for water desalination. *Desalination* **2015**, *368*, 106–113. [[CrossRef](#)]
93. Bano, S.; Mahmood, A.; Kim, S.; Lee, K. Graphene oxide modified polyamide nanofiltration membrane with improved flux and antifouling properties. *J. Mater. Chem.* **2015**, *3*, 2065–2071. [[CrossRef](#)]
94. Al Hobibi, A.S.; Ghoul, J.; Chiloufi, I.; EL Mir, L. Synthesis and characterization of polyamide thin film nanocomposite membrane reached by aluminum doped ZnO. *Mater. Sci. Semicond. Process.* **2016**, *42*, 111–114. [[CrossRef](#)]
95. Liu, L.; Zhu, G.; Liu, Z.; Gao, C. Effect of MCM-48 nanoparticles on the performance of TFN membrane for reverse osmosis application. *Desalination* **2016**, *394*, 72–82. [[CrossRef](#)]
96. Yin, J.; Deng, B. Graphene oxide enhanced polyamide thin-film nanocomposite membrane for water purification. *Desalination* **2016**, *379*, 93–101. [[CrossRef](#)]
97. Mayyahi, A.A.; Deng, B. Efficient water desalination using photo-responsive ZnO polyamide thin film nanocomposite membrane. *Environ. Chem. Lett.* **2018**, 1–7. [[CrossRef](#)]
98. Kadhom, M.; Deng, B. Thin film nanocomposite membrane filled with metal-organic frameworks UiO-66 and MIL-125 nanoparticles for water desalination. *Membrane* **2017**, *7*, 31. [[CrossRef](#)] [[PubMed](#)]
99. Bi, R.; Zhang, Q.; Zhang, R.; Su, Y.; Jiang, Z. Thin Film Nanocomposite Membranes Incorporated with Graphene Quantum Dots for High Flux and Antifouling Property. *J. Membr. Sci.* **2018**, *553*, 17–24. [[CrossRef](#)]
100. Aljundi, I.H. Desalination characteristics of TFN-RO membrane incorporated with ZIF-8 nanoparticles. *Desalination* **2017**, *430*, 12–20. [[CrossRef](#)]
101. Khorshidi, B.; Biswas, I.; Ghosh, T.; Thundat, T.; Sadzadeh, M. Robust fabrication of thin film polyamide-TiO₂ nanocomposite membranes with enhanced thermal stability and anti-biofouling propensity. *Sci. Rep.* **2018**, *8*, 784. [[CrossRef](#)] [[PubMed](#)]
102. Sun, H.; Wu, P. Tuning the functional groups of carbon quantum dots in thin film nanocomposite membranes for nanofiltration. *J. Membr. Sci.* **2018**, *564*, 394–403. [[CrossRef](#)]
103. He, Y.; Zhao, D.L.; Chung, T.S. Na⁺ functionalized carbon quantum dot incorporated thin-film nanocomposite membranes for selenium and arsenic removal. *J. Membr. Sci.* **2018**, *564*, 483–491. [[CrossRef](#)]

104. Peyki, A.; Rahimpour, A.; Jahanshahi, M. Preparation and characterization of thin film composite reverse osmosis membranes incorporated with hydrophilic SiO₂ nanoparticles. *Desalination* **2015**, *368*, 152–158. [[CrossRef](#)]
105. Ma, D.; Peh, S.P.; Han, G.; Chen, S.B. Thin-Film Nanocomposite (TFN) Membranes Incorporated with Super-Hydrophilic Metal–Organic Framework (MOF) UiO-66: Toward Enhancement of Water Flux and Salt Rejection. *ACS Appl. Mater. Interfaces* **2017**, *9*, 7523–7534. [[CrossRef](#)] [[PubMed](#)]
106. Mayyahi, A.A. Thin-film composite (TFC) membrane modified by hybrid ZnO-graphene nanoparticles (ZnO-Gr NPs) for water desalination. *J. Environ. Chem. Eng.* **2018**, *6*, 1109–1117. [[CrossRef](#)]
107. Rajaeian, B.; Rahimpour, A.; Tade, M.O. Fabrication and characterization of polyamide thin film nanocomposite (TFN) nanofiltration membrane impregnated with TiO₂ nanoparticles. *Desalination* **2013**, *313*, 176–188. [[CrossRef](#)]
108. Glater, J.; Hong, S.; Elimelech, M. The search for a chlorine-resistance reverse osmosis membrane. *Desalination* **1994**, *95*, 325–345. [[CrossRef](#)]
109. Xue, S.X.; Ji, C.H.; Xu, Z.L.; Tang, Y.J.; Li, R.H. Chlorine resistant TFN nanofiltration membrane incorporated with octadecylamine-grafted GO and fluorine-containing monomer. *J. Membr. Sci.* **2018**, *545*, 185–195. [[CrossRef](#)]
110. Nikolova, J.D.; Islam, M.A. Contribution to adsorbed layer resistance to flux decline in ultrafiltration process. *J. Membr. Sci.* **1998**, *146*, 105–111. [[CrossRef](#)]
111. Sadar Ghayeni, S.B.; Beatson, P.J.; Schneider, R.P.; Fane, A.G. Adhesive of water bacteria to reverse osmosis membrane. *J. Membr. Sci.* **1998**, *138*, 29–42. [[CrossRef](#)]
112. Kim, E.-S.; Deng, B. Fabrication of polyamide thin-film-nano-composite (PA-TFN) membrane with hydrophilized ordered mesoporous carbon for water purification. *J. Membr. Sci.* **2011**, *375*, 46–54. [[CrossRef](#)]
113. Lee, S.; Kim, H.; Patel, R.; Im, S.; Kim, J.; Min, B. Silver nanoparticles immobilized on thin film composite polyamide membrane: characterization, nanofiltration, antifouling properties. *Polym. Adv. Tech.* **2007**, *18*, 562–568. [[CrossRef](#)]
114. Sondi, I.; Sondi, B. silver nanoparticles as antimicrobial agent: A case study on E. Coil as a model for gram-negative bacteria. *J. Colloid Interface Sci.* **2004**, *275*, 177–182. [[CrossRef](#)] [[PubMed](#)]
115. Park, M.; Neigh, A.; Vermeulen, J.; Fonteyne, L.; Verharen, H.; Briede, J.; Loveren, H.; Jong, W. The effect of particle size on the cytotoxicity, inflammation, development of toxicity and genotoxicity of silver nanoparticles. *Biomaterials* **2011**, *36*, 9810–9817. [[CrossRef](#)] [[PubMed](#)]
116. Ben-Sasson, M.; Zodrow, K.R.; Genggeng, Q.; Kang, Y.; Giannelis, E.P.; Elimelech, M. Surface functionalization of thin-film composite membranes with copper nanoparticles for antimicrobial surface properties. *Environ. Sci. Technol.* **2014**, *48*, 384–393. [[CrossRef](#)] [[PubMed](#)]
117. Kim, S.; Kwak, S.; Sohn, B.; Park, T. design of TiO₂ nanoparticles self-assembled aromatic polyamide thin-film composite (TFC) membrane as an approach to solve biofouling problem. *J. Membr. Sci.* **2003**, *211*, 157–165. [[CrossRef](#)]
118. Choi, W.; Choi, J.; Bang, J.; Lee, J.H. Layer-by-layer assembly of graphene oxide nanosheets on polyamide membranes for durable reverse-osmosis applications. *ACS Appl. Mater. Interfaces* **2013**, *5*, 12510–12519. [[CrossRef](#)] [[PubMed](#)]
119. Hu, M.; Mi, B. Enabling graphene oxide nanosheets as water separation membranes. *Environ. Sci. Technol.* **2013**, *47*, 3715–3723. [[CrossRef](#)] [[PubMed](#)]
120. Yin, J.; Yang, Y.; Hu, Z.; Deng, B. Attachment of silver nanoparticles (AgNPs) onto thin-film composite (TFC) membranes through covalent bonding to reduce membrane biofouling. *J. Membr. Sci.* **2013**, *441*, 73–82. [[CrossRef](#)]
121. Mayyahi, A.A. TiO₂ polyamide thin film nanocomposite reverses osmosis membrane for water desalination. *Membranes* **2018**, *8*, 66. [[CrossRef](#)]

